Assessment of reinforced overlay for masonry retrofitting: lime vs cementitious plaster

Manuela Scamardo[1*], *Sara* Cattaneo[1], and *Pietro* Crespi[1]

[1]Politecnico di Milano, ABC Department, Milano, Italy

Abstract. Reinforced overlay is a very common retrofitting technique adopted in existing masonry buildings to improve their performance under seismic action, both in-plane and out-of-plane. The most traditional and widespread approach considers the use of cementitious mortar as plaster with steel meshes as reinforcement. However, cementitious materials may raise compatibility problems with the base material and sustainability issues, thus the use of lime mortar should be preferred. This paper presents the results of an experimental program aimed at assessing the contribution of the reinforced plaster strengthening system in increasing the load carrying capacity of masonry walls, comparing the performance of cementitious and lime mortar plaster. Cyclic diagonal compression tests were performed under displacement control. Unreinforced specimens were also tested as reference for the improvement evaluation. The results showed an improved performance with respect to the unreinforced ones for both the materials (cementitious and lime mortar), in terms of both strength and deformation capacity. The peak load seemed to be not significantly affected by the type of plaster, while higher displacement at the ultimate load was observed in case of lime mortar. Finally, an analytical method formulated to predict the strength of walls retrofitted with cementitious reinforced plaster was applied to check its validity also in case of lime-based plaster.

1 Introduction

Unreinforced masonry structures were usually built in the past under empirical rules to resist only to vertical loading. For this reason, most of them result vulnerable to lateral loads such as that imposed by earthquakes [1–3], requiring strengthening interventions to guarantee the structural safety and limit the economic and human losses after seismic events.

In the last few decades, different retrofitting techniques have been developed and implemented to improve the behaviour of masonry buildings under seismic actions [4–6], using more conventional approaches (e.g. shotcrete, grout injections) [7,8] or introducing innovative materials (e.g., fiber-reinforced polymers grid or strips) [9–11]. The choice of the most appropriate retrofitting method should be made by carefully considering several factors:

* Corresponding author: manuela.scamardo@polimi.it

These proceedings are published with the support of EuLA.

(i) cost, (ii) sustainability, (iii) compatibility, (iv) durability and, in case of historical heritage structures, (v) reversibility and (vi) minimum intervention.

Among the most conventional approaches, steel reinforced plaster (SRP) has been widely adopted thanks to its ability to enhance strength, stiffness, and deformation capacity of masonry, both in the in-plane and out-of-plane behaviour, with limited cost and easy application. Furthermore, the method is recommended as an effective retrofitting technique by several Design Codes [12–15].

The plaster coating has a thickness commonly ranging from 30 to 80 mm and is typically realized with cement-based mortar. However, applications with lime-based mortar have been introduced, with several benefits such as superior compatibility with the masonry substrate, transpirability (which avoids moisture problems), and higher sustainability with respect to the cement one [16]. Indeed, lime mortar is a natural carbon-neutral building material while the cement production is a highly energy-intensive process that releases a lot of greenhouse gases into the atmosphere.

Despite the widespread use of SRP, it is difficult to find a proper mechanical characterization of the method in the scientific literature and only few studies have been published with limited experimental data [17–19]. For this reason, an experimental research has been conducted on unreinforced and SRP-retrofitted masonry specimens subjected to diagonal compression tests to investigate their behaviour under cyclic loads, considering the use of cement-based or lime-based reinforced plaster. Additional design parameters were also investigated such us plaster thickness and number of connectors. The paper presents and discusses the experimental outcomes, analysing the effect of the plaster type on the masonry performance.

2 Experimental research

2.1 Specimens and materials

The tested masonry specimens had dimensions of 1290x1290 mm and thickness of 250 mm, and were made by clay bricks arranged in English bond (Fig. 1a). The average compressive strength of the bricks was 23.3 MPa, while the average elastic modulus was 2207 MPa. For bed joints, a M2.5 lime-cement mortar was used, with 1:5 water/cement ratio by weight. The mean value of mortar compressive strength was 5.4 MPa.

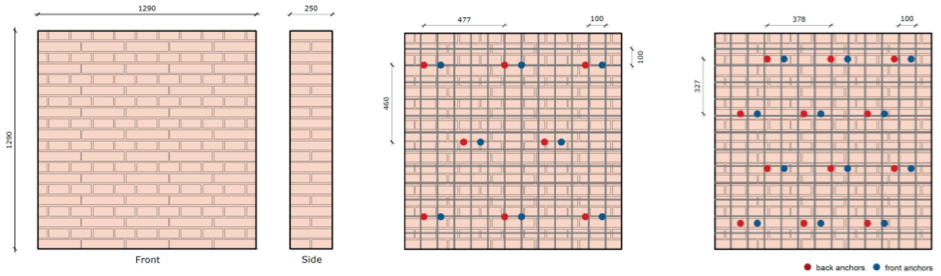

(a) (b) (c)

Fig. 1. Geometry of masonry specimen (a) and reinforcement configuration with 8 (b) and 12 (c) anchors.

In the retrofitted configuration, a plaster overlay was applied on both sides of the specimen. A steel mesh of 6 mm diameter wire (B450C class), with a spacing of 100 mm in both horizontal and vertical directions, was used as reinforcement. Steel anchors in the form

of steel ribbed rebars (B450C, 8 mm diameter, 200 mm embedment depth), bent at one end with a 90-degree hook of length 50 mm, were used to connect the plaster cover to the masonry. A hybrid adhesive was used to install the connectors into boreholes (diameter 10 mm) with a quincunx pattern. Two different anchors layout were considered, with 8 anchors per side (Fig.1b) or 12 (Fig.1c). The plaster overlay was realized with a cement-based mortar with compressive strength of 33.8 MPa, or with a lime-based mortar with compressive strength of 18.9 MPa, considering two different thickness (i.e. 30 and 50 mm).

A total of 10 specimens were tested (2 unreinforced), in two subsequent experimental campaign. The first set of tests included the unreinforced specimens and the cement-based retrofitted ones [20]; the second set included the specimens retrofitted with lime-based plaster. Since the coefficient of variation for the retrofitted specimens of the first set was very low (about 3%), in the second set of tests only one specimen for each configuration was tested. Table 1 summarizes the performed test program, with the main characteristic of the specimen for each configuration, the number of repetitions, and the identification code (M: masonry, U/R: unreinforced or retrofitted, number of wythes (2 or 3), thickness of the plaster in cm, number of anchors, C/L cementitious or lime mortar).

Table 1. Test program, code and specimen characteristics.

Code	Wall			Reinforced plaster			#repeats
	Width (mm)	Height (mm)	Thickness (mm)	Thickness (mm)	Mortar type	#anchors	
MU2	1290	1290	250	-	-	-	2
MR2-3-8-C				30	Cem	8	2
MR2-5-8-C				50	Cem	8	2
MR2-3-8-L				30	Lime	8	1
MR2-3-12-L				30	Lime	12	1
MR2-5-8-L				50	Lime	8	1
MR2-5-12-L				50	Lime	12	1

2.2 Test set-up and procedure

Diagonal compression tests were performed on the masonry specimens according to the ASTM E519 Standard [21]. The load was applied by means of two hydraulic jacks (capacity of 300 kN each) placed diagonally on both sides of the specimen (Fig. 2a, 2b). Two load cells (capacity of 300 kN each) were used to constantly monitor the load. The displacement applied by the hydraulic jacks was transferred to the wall corners using two L-shaped steel shoes.

The tests were performed under displacement control. The displacement along the diagonals was monitored using linear variable differential transformers (LVDTs) with gauge length of about 800 mm, two for each side of the wall. For the strengthened specimens, two additional LVDTs per side was placed orthogonally to the wall front/back face to monitor the out-of-plane deformation. The LVDTs layout is shown in Fig. 2c.

The displacement protocol proposed by Porter [22] was adopted which considers two main phases: (i) application of monotonic load until the first crack is detected, i.e., first major event (FME); (ii) application of cyclic displacement history, defined on the basis of the displacement associated to the FME. The first 10 increasing cycles are defined as the 25% (3 cycles), 50% (3 cycles) and 75% (3 cycles) of the FME displacement, plus a final cycle at 100%. The unloading is then performed with 3 decreasing cycles. The displacement is then stabilized by applying 3 cycles at 100%. If the load decrease between two successive cycles

is less than 5%, the system is considered stable. The protocol proceeds with one cycle at 125% FME, 3 progressive unloading cycles and 3 stabilizing cycles at 125% FME. The sequence is then repeated by increasing each time the target FME percentage by 25%. The displacement protocol is reported in Figure 3.

It should be underlined that, due to damage developed during cycles, it was not always possible to reach the original jack position with the consequent recording of residual stroke after a certain displacement level.

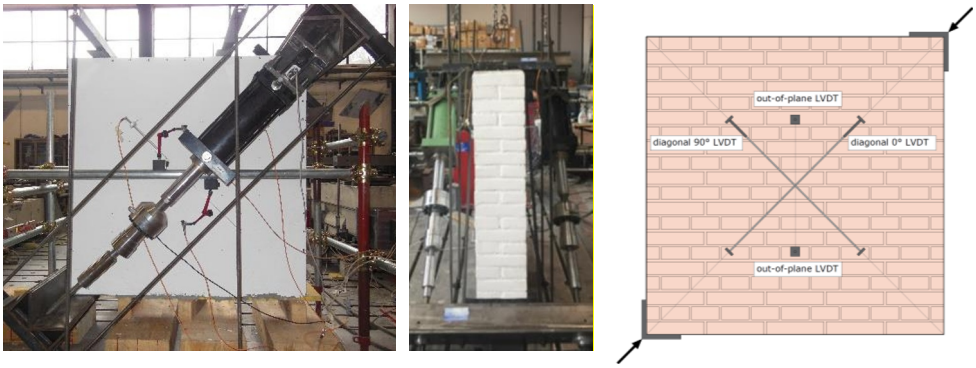

(a) (b) (c)

Fig. 2. Test set-up: (a) front view, (b) side view and (c) LVDT's layout.

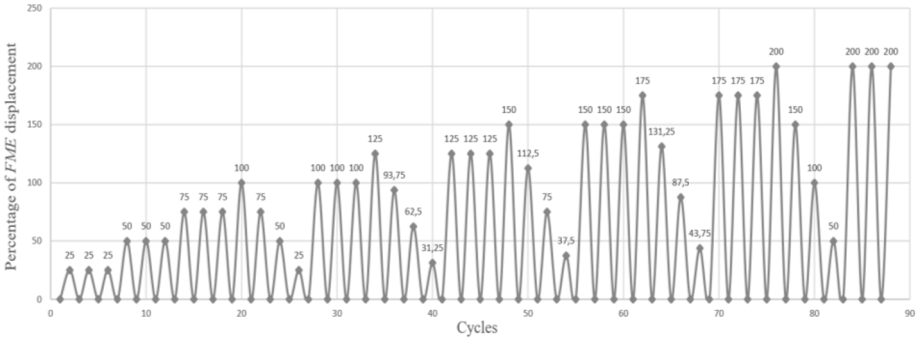

Fig. 3. Cyclic SPD protocol.

2.3 Test results

Table 2 summarizes the main results of the experimental tests. In particular, the load and the stroke (displacement of the jacks) associated to the FME, to the peak (ultimate load), and to the final failure (residual load) of the specimen are reported, together with the percentage of FME at the peak and at the final failure and the area of the hysteresis loops. The ultimate and residual loads are also plotted in Figure 4 vs. the stroke (a) and the strain (b). The stroke associated to the FME in the tests with lime plaster was assumed equal to 6.58 mm on the basis of the mean FME strokes recorded for the unreinforced specimens and the ones with cementitious plaster.

In general, in terms of ultimate load, the lime-based plaster was able to reach the capacity of the cementitious plaster, and, in some cases, also to overcome it (i.e. MR2-5-8-L, MR2-5-12-L) with an increase of the load of about 36% with respect to the cementitious one. The

residual load and areas of the hysteresis loop resulted comparable. The stroke at the ultimate load resulted instead always higher in the case of the lime plaster (range 18.98-27.75 mm) with respect to the cement-based one (range 11.69-13.32 mm).

Table 2. Test results.

Code	FME		Maximum load			Residual load			Area of hysteresis loop
	Load	Stroke	Load	Stroke	%FME	Load	Stroke	%FME	
	kN	mm	kN	mm	-	kN	mm	-	kNmm
MU2-1	199.13	6.58	232.22	7.48	114%	-	-	-	733.9
MU2-2	-	-	165.12	5.69	87%	-	-	-	519.5
MR2-3-8-C-1	202.54	5.69	366.80	12.64	222%	112.46	21.43	377%	3890.1
MR2-3-8-C-2	-	-	372.45	13.32	234%	157.98	31.06	546%	5720.1
MR2-5-8-C-1	277.17	8.17	376.63	11.69	143%	208.53	38.50	471%	7247.2
MR2-5-8-C-2	-	-	373.97	13.14	161%	164.24	44.51	545%	7735.7
MR2-3-8-L	-	-	363.25	27.75	422%	94.70	38.04	579%	5409.7
MR2-3-12-L	-	-	344.14	18.98	289%	215.78	45.60	693%	7536.2
MR2-5-8-L	-	-	497.84	19.11	291%	165.86	26.48	403%	6935.8
MR2-5-12-L	-	-	509.37	22.08	336%	199.72	29.46	448%	7414.2

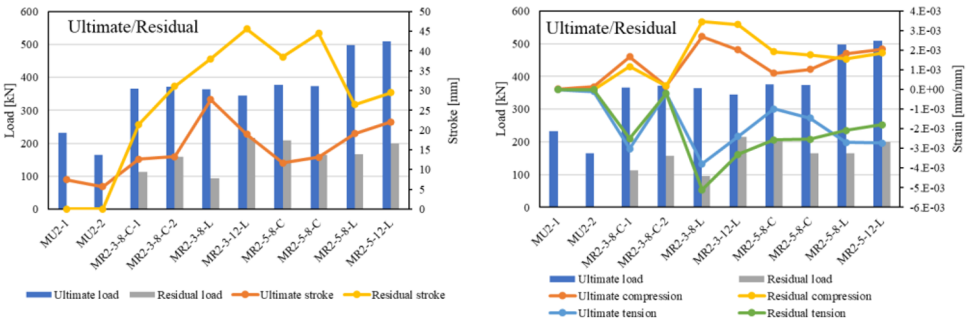

(a) (b)

Fig. 4. Ultimate/residual loads vs. stroke (a) and vs. strain (b).

3 Discussion

In order to better understand the different behaviour of cement and lime-based plasters, Figure 5 shows the comparison in terms of load vs. displacement curves for 3 cm plaster (a) and 5 cm plaster (b). The curve of the unreinforced configuration is also reported as reference. It can be noted that, in the case of plaster thickness of 3 cm, there is only a small variation in terms of peak loads between cementitious and lime plasters. On the contrary, in the case of plaster thickness of 5 cm, the lime mortar allows a significant increase of the peak load with respect to cementitious mortar. However, this latter showed a better behaviour after the peak, being able to maintain a certain load for several cycles, after an initial load decrease. In case of lime plaster, the behaviour after the peak resulted more brittle, with a sudden drop of the load (associated to the detachment of one side of the plaster). Additionally, the lime plaster always results in higher displacement at the peak. In general, it is evident that the higher

plaster thickness has positive effects in terms of higher post-peak ductility for the cementitious plaster, and higher load bearing capacity in the case of the lime plaster.

Different failure patterns were detected for the different plaster types (Fig. 6 and Fig, 7). In the case of cementitious one, fine multiple cracks were detected on a wide area along the loaded diagonal, with crushing of the plaster at the loaded corners (Fig. 6a). Close to the peak load, the plaster cover detached from the substrate (Fig. 6b). In the post peak phase, punching of the plaster was also observed due to the anchors bending. At the end of the test, after the removal of the plaster layer, the masonry resulted interested by multiple cracks, crossing both brick and mortar (Fig.6c).

In case of lime plaster, thin multiple cracks were also detected on a wide area along the loaded diagonal (Fig. 7a). The plaster crushing at corners was more evident due to the lower strength of the plaster (Fig, 7b), with significant loss of material (spalling) such that, at a certain point of the test, the load was applied directly to the top part of the masonry wall. Probably for this reason, a sliding of the first 2 or 3 rows of bricks was observed in some of the tests (Fig. 7c). Additionally, the plaster punching was observed only in few cases in the specimens with 3 cm plaster, while it was not observed at all in the case of 5 cm plaster.

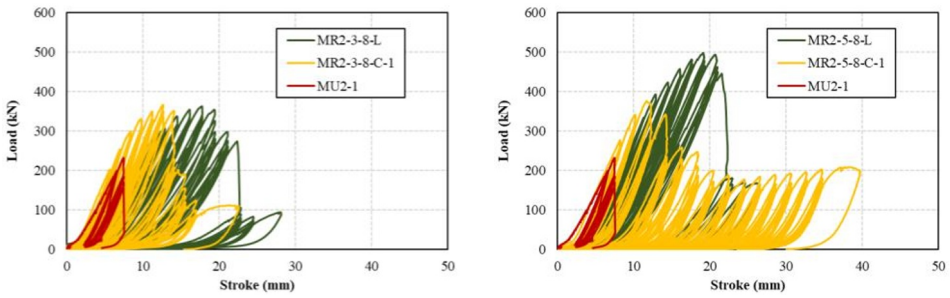

(a) (b)

Fig. 5. Load vs. displacement curves for cementitious and lime plaster with different thickness: (a) 3 cm and (b) 5 cm.

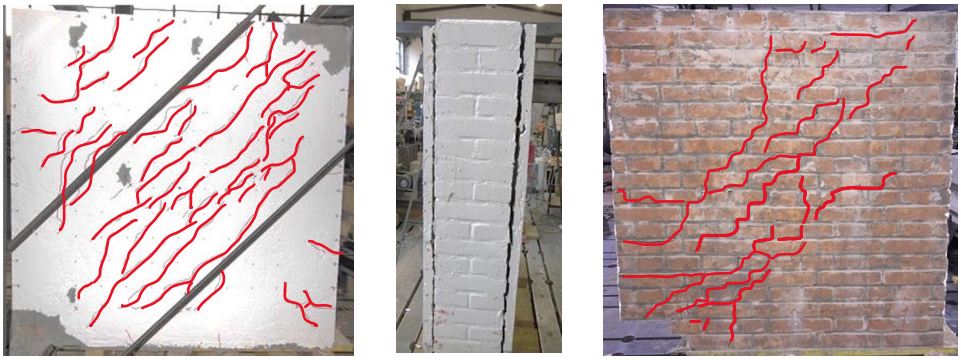

(a) (b) (c)

Fig. 6. Damage pattern at the end of the test for cementitious plaster specimen MR2-3-8-C-1: (a) front, (b) side and (c) on masonry behind the plaster.

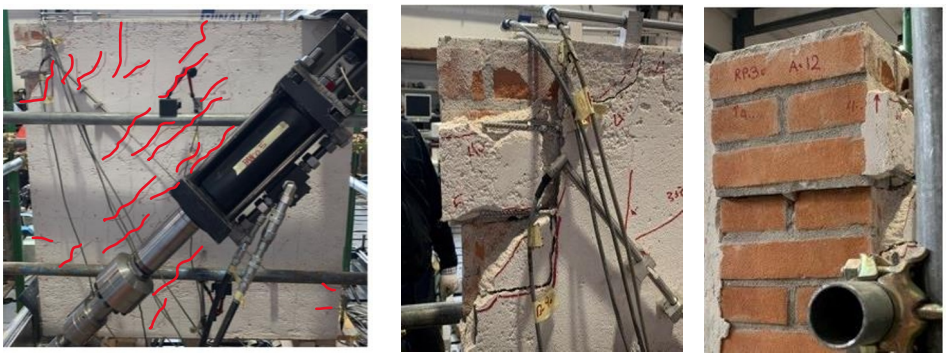

(a) (b) (c)

Fig. 7. Damage pattern at the end of the test for lime plaster specimen MR2-3-12-L: (a) front, (b) corner and (c) sliding of the masonry bricks.

Figure 8 reports the comparison in terms of load vs. displacement curves for different number of anchors in case of lime plaster with 3 cm (a) or 5 cm (b) thickness. In the configurations considered, the number of anchors does not affect significantly the load capacity, but it increases the stiffness and the ductility of the structure. It should be also highlighted that, during the tests, a higher number of anchors resulted in a late detachment of the plaster layers, with more limited out-of-plane displacements.

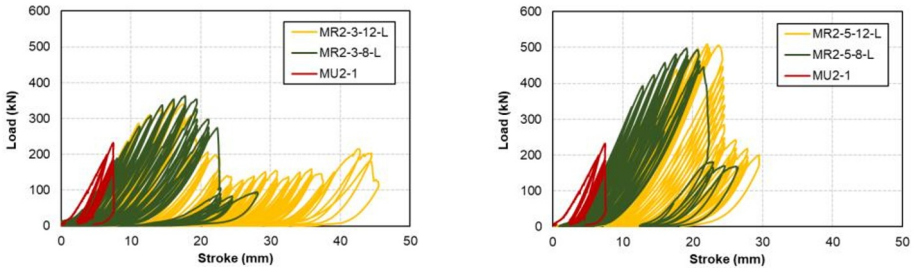

(a) (b)

Fig. 8. Load vs. displacement curves for cementitious and lime plaster with different thickness: (a) 3 cm and (b) 5 cm.

4 Analytical evaluations

The analytical approach for the prediction of the failure load of masonry wall retrofitted with SRP proposed by Scamardo et al. [23] has been used to make some additional considerations. The approach was calibrated and validated using experimental results of specimens retrofitted with cement-based plaster [20]. The aim is to check its validity also in case of lime-based plaster.

The method accounts for the main parameters affecting the performance of the strengthened wall such as the masonry properties, the plaster properties and the spacing and number of connectors. The approach takes into account two possible plaster failure mechanisms under diagonal compression, i.e. crushing and instability of the plaster layer (possible after the plaster detachment from the masonry substrate). The masonry wall is studied as a diagonal strut with length L_d equal to the diagonal length of the wall, and width

$w = 0.15L_d$. The ultimate load N_{max} is evaluated as the sum of the contribution provided by the masonry and the one given by each plaster layer as:

$$N_{max} = \min\left\{2N_{p,i} + N_m, 2N_{p,c} + N_m\right\} \quad (1)$$

where N_m is the maximum load in masonry, while $N_{p,i}$ and $N_{p,c}$ are the maximum load in each plaster layer associated to the instability and crushing failure, respectively.
The masonry strut maximum load N_m is evaluated as:

$$N_m = f_m \cdot w \cdot t_m \quad (2)$$

with f_m masonry compressive strength and t_m masonry thickness.
The limit load $N_{p,c}$ associated with the crushing of the plaster is calculated as:

$$N_{p,c} = f_{c,r} \cdot w \cdot t_p \quad (3)$$

where t_p is the plaster layer thickness and $f_{c,r}$ is its compressive strength, reduced to take into account the effect of shear cracks on the compressive resistance.
The limit load $N_{p,i}$ associated with the buckling failure of the plaster is calculated as:

$$N_{p,i} = i \cdot P_{cr} \quad (4)$$

where P_{cr} is the critical buckling load of the plaster strut, which takes into account also the stiffness and number of connectors, and i is a coefficient to account for the presence of initial imperfections (e.g., construction imperfections, eccentricity of the load). For further details see [23].
Table 3 reports the experimental (P_{exp}) and analytical (N_{max}) ultimate load for comparison, and the required input parameters: L is the side dimension of the masonry specimen, t_m is the wall thickness, f_m is the mean masonry compressive strength, t_p is the plaster thickness, f_c is the mean plaster compressive strength, n is the number of connectors per square meters. In the last column the percentage change of the analytical result with respect to the experimental one is reported as well. When more experimental tests were available for a certain configuration, the mean value of P_{exp} is reported.

It should be highlighted that the only parameter which depends on the type of plaster mortar (cementitious or lime) is the plaster compressive strength f_c.

Table 3. Input parameters, experimental (P_{exp}) and analytical (P_{an}) ultimate loads.

Code	L (mm)	t_m (mm)	f_m (MPa)	t_p (mm)	f_c (MPa)	n (1/m²)	P_{exp} (kN)	N_{max} (kN)	±%
MU2	1290	250	3.08	-	-	-	198.7	211.0	+6%
MR2-3-8-C	1290	250	3.08	30	33.8	4.8	369.6	356.0	-4%
MR2-5-8-C	1290	250	3.08	50	33.8	4.8	375.3	508.0	+26%
MR2-3-8-L	1290	250	3.08	30	18.9	4.8	363.3	340.2	-7%
MR2-3-12-L	1290	250	3.08	30	18.9	7.21	344.1	354.3	+3%
MR2-5-8-L	1290	250	3.08	50	18.9	4.8	497.8	475.6	-5%
MR2-5-12-L	1290	250	3.08	50	18.9	7.21	509.4	505.9	-1%

The results shows that the analytical model is able to well predict the experimental evidence. The percentage change related to the test MR2-5-8-C shows the highest error (+26%). However, this experimental result was unexpected and considered as an outlier (see [20]). Neglecting this value, the percentage change for the retrofitted specimens ranges reasonably between -7% and +3%, proving the validity of the approach also in case of lime-based plaster.

5 Conclusions

The paper presented and discussed the results of an experimental program of diagonal tests conducted on masonry specimens retrofitted with steel reinforced plaster. The aim was to analyse and compare the performance obtained using cement-based or lime-based plaster as overlay. The main outcomes are summarized in the following:

- the performance of lime plaster, in terms of load bearing capacity, resulted at least equivalent to the cementitious one, and in same cases (5 cm plaster thickness) superior;
- the specimens reinforced with lime plaster showed lower stiffness with respect to the cementitious plaster ones, with higher displacement at the ultimate load and a brittle post peak behaviour;
- the dissipation capacity (areas of hysteresis loop) of the two types of plaster resulted similar; however, the cementitious plaster was able to maintain a certain load after the peak, while, in the case of the lime one, a sudden drop of the loas was usually observed after the peak;
- the analytical method previously presented by the authors for the prediction of the load capacity of masonry walls retrofitted with cementitious reinforced plaster resulted also valid for lime-based reinforced plaster.

It should be underlined that the presented results are related to a reduced number of tests, with limited variations of the investigated parameters. Therefore, the drawn conclusions should be limited to the studied configurations. Further experiments should be performed to confirm the observed trend and examine in depth the effects of the lime plaster on the masonry performance.

References

1. A. Penna, C. Calderini, L. Sorrentino, C.F. Carocci, E. Cescatti, R. Sisti, A. Borri, C. Modena, A. Prota, Damage to churches in the 2016 central Italy earthquakes, Bulletin of Earthquake Engineering **17** (2019). https://doi.org/10.1007/s10518-019-00594-4.
2. G. Fiorentino, A. Forte, E. Pagano, F. Sabetta, C. Baggio, D. Lavorato, C. Nuti, S. Santini, Damage patterns in the town of Amatrice after August 24th 2016 Central Italy earthquakes, Bulletin of Earthquake Engineering **16** (2018) 1399–1423. https://doi.org/10.1007/s10518-017-0254-z.
3. İ. Kocaman, The effect of the Kahramanmaraş earthquakes (Mw 7.7 and Mw 7.6) on historical masonry mosques and minarets, Eng Fail Anal **149** (2023). https://doi.org/10.1016/j.engfailanal.2023.107225.
4. S. Bhattacharya, S. Nayak, S.C. Dutta, A critical review of retrofitting methods for unreinforced masonry structures, International Journal of Disaster Risk Reduction **7** (2014) 51–67. https://doi.org/10.1016/j.ijdrr.2013.12.004.
5. M. Scamardo, M. Zucca, P. Crespi, N. Longarini, S. Cattaneo, Seismic Vulnerability Evaluation of a Historical Masonry Tower: Comparison between Different

Approaches, Applied Sciences (Switzerland) **12** (2022). https://doi.org/10.3390/app122111254.

6. G. Cianchino, M.G. Masciotta, C. Verazzo, G. Brando, An Overview of the Historical Retrofitting Interventions on Churches in Central Italy, Applied Sciences (Switzerland) **13** (2023). https://doi.org/10.3390/app13010040.
7. M.A. Elgawady, P. Lestuzzi, A review of conventional seismic retrofitting techniques for URM, 13th International Brick and Block Masonry Conference, Amsterdam, July 4-7, 2004 (2004) 1–10.
8. S.R.S. Rezaee, M. Soltani, M. Nikooravesh, Cyclic in-plane behavior of unreinforced and confined masonry walls retrofitted by shotcrete: Experimental investigation, Eng Struct **264** (2022). https://doi.org/10.1016/j.engstruct.2022.114432.
9. S. Casacci, C. Gentilini, A. Di Tommaso, D. V. Oliveira, Shear strengthening of masonry wallettes resorting to structural repointing and FRCM composites, Constr Build Mater **206** (2019) 19–34. https://doi.org/10.1016/J.CONBUILDMAT.2019.02.044.
10. S. Cattaneo, P. Crespi, M. Scamardo, N. Vafa, Cyclic behavior of masonry walls retrofitted with post-installed twisted bars or bonded rebars, Constr Build Mater **409** (2023). https://doi.org/10.1016/j.conbuildmat.2023.134026.
11. M. Jarc Simonič, S. Gostič, V. Bosiljkov, R. Žarnić, In-situ and laboratory tests of old brick masonry strengthened with FRP in innovative configurations and design considerations, Bulletin of Earthquake Engineering **13** (2015) 257–278. https://doi.org/10.1007/s10518-014-9644-7.
12. Ministero delle infrastrutture e dei Trasporti, Decreto Ministeriale 17 Gennaio 2018 C.S.LL.PP. Aggiornamento delle «Norme tecniche per le costruzioni», (2018).
13. Ministero delle Infrastrutture e dei Trasporti, Circolare 21 gennaio 2019, n. 7 C.S.LL.PP. Istruzioni per l'applicazione dell'«Aggiornamento delle Norme tecniche per le costruzioni», (2019) 1–14.
14. Eartquake planning and protection organization (E.E.P.O.), KAN.EPE. Code of interventions on reinforced concrete buildings, English version after harmonization with Eurocode 8, Part 3, (2013) 1–337.
15. Federal Emergency Management Agency, American Society of Civil Engineers, FEMA 356 Prestandard and commentary for the seismic rehabilitation of buildings, 2000.
16. Z. Chen, H. Liu, L. Xu, W. Ge, A review of mechanical properties and carbonation behavior evolution of lime mortar for architectural heritages restoration, Minerals and Mineral Materials **3** (2024). https://doi.org/10.20517/mmm.2023.26.
17. S. Churilov, E. Dumova-Jovanoska, In-plane shear behaviour of unreinforced and jacketed brick masonry walls, Soil Dynamics and Earthquake Engineering **50** (2013) 85–105. https://doi.org/10.1016/j.soildyn.2013.03.006.
18. B. Ghiassi, M. Soltani, A.A. Tasnimi, Seismic Evaluation of Masonry Structures Strengthened with Reinforced Concrete Layers, (2012). https://doi.org/10.1061/(ASCE)ST.1943-541X.
19. G. Maddaloni, Analisi sperimentale del comportamento di edifici in muratura rinforzati con tecniche e materiali innovativi, PhD Thesis, 2017.
20. L. Biolzi, S. Cattaneo, P. Crespi, M. Scamardo, N. Vafa, Diagonal compression cyclic testing of unreinforced and reinforced masonry walls, Constr Build Mater **363** (2023).

21. ASTM International, ASTM E519 - Standard Test Method for Diagonal Tension (Shear) in Masonry Assemblages, 2021. https://doi.org/10.1520/E0519.
22. M.L. Porter, Sequential Phased Displacement (SPD) Procedure for TCCMAR Testing, in: Third Meeting of the Joint Technical Coordinating Committee on Masonry Research, U.S. - Japan Coordinated Earthquake Research Program, Tomamu, Japan, 1987.
23. M. Scamardo, S. Cattaneo, P. Crespi, L. Biolzi, Design method for masonry structures retrofitted with steel reinforced plaster, Journal of Building Engineering **79** (2023). https://doi.org/10.1016/j.jobe.2023.107828.